Atmospheric fate of organosulfates through gas-phase and aqueous-phase reaction with hydroxyl radicals: implications in inorganic sulfate formation

Narcisse Tsona Tchinda[1], Xiaofan Lv[1], Stanley Numbonui Tasheh[2], Julius Numbonui Ghogomu[2,3], Lin Du[1]

[1]Qingdao Key Laboratory for Prevention and Control of Atmospheric Pollution in Coastal Cities, Environment Research Institute, Shandong University, Qingdao, 266237, China
[2]Department of Chemistry, Faculty of Science, The University of Bamenda, P.O. Box 39 Bambili-Bamenda, Cameroon
[3]Research Unit of Noxious Chemistry and Environmental Engineering, Department of Chemistry, Faculty of Science, University of Dschang, P.O. Box 67 Dschang, Cameroon

Correspondence to: Narcisse Tsona Tchinda (tsonatch@sdu.edu.cn) and Lin Du (lindu@sdu.edu.cn)

Abstract. Organosulfates are important tracers for aerosol particles, yet their influence on aerosol chemical composition remains poorly understood. This study uses quantum chemical calculations based on density functional theory to explore the reactions of some prevalent organosulfates, specifically methyl sulfate and glycolic acid sulfate, with hydroxyl radicals (HO•) in the gas-phase and aqueous-phase. Results indicate that all reactions initiate with hydrogen abstraction by HO• from CH_3- in methyl sulfate and from -CH_2- and -COOH in glycolic acid sulfate, followed by the further reaction of the resulting radicals through self-decomposition, interaction with O_2 and, possibly, O_3. We found that the hydrogen abstraction from the -COOH group in glycolic acid sulfate could lead to decarboxylation and eventually form similar products as methyl sulfate. The primary reaction products are inorganic sulfate, carbonyl compounds and formic sulfuric anhydride. Rate constants of 1.14×10^{-13} cm^3 $molecule^{-1}$ s^{-1} and 6.17×10^{-12} cm^3 $molecule^{-1}$ s^{-1} at 298.15 K were determined for the gas-phase reaction of methyl sulfate and glycolic acid sulfate, respectively. The former value is consistent with a previous experimental report. Additionally, while prior studies suggested O_2 as primary oxidant in the fragmentation of organosulfates, this study unveils O_3 as a complementary oxidant in the intermediate steps of this process. Overall, this study elucidates mechanisms for HO•-initiated transformation of organosulfates and highlights the potential role of chemical substitution, thereby enhancing our understanding of their atmospheric chemistry and implication for inorganic sulfate formation, which are vital for evaluating their impact on aerosol properties and climate processes.

1 Introduction

Atmospheric particulate matter is a complex mixture of inorganic and organic matter, with organic matter typically accounting for 20-90% of the total mass (Hallquist et al., 2009; Stone et al., 2012). The concentration level of particulate matter and its evolution have important impacts on regional air quality, climate change and human health. In this regard, the study of organic

aerosol concentration levels, sources, and secondary transformations is key to understanding the formation mechanism of compounds responsible for air pollution. Organosulfates, characterized by sulfate groups ($R\text{-}OSO_3H/R\text{-}OSO_3^-$, where R is an alkyl or aryl group), constitute the most abundant component of organic aerosols. Organosulfates have been widely detected in aerosol particles from various environments in the Americas, Europe, Asia, and the Arctic over the past decades (Iinuma et al., 2007; Surratt et al., 2008; Nguyen et al., 2014; Kourtchev et al., 2016; Lin et al., 2014). Due to the presence of $-OSO_3^-$ or $-OSO_3H$ functional group in their structure, organosulfates are acidic and highly water-soluble, which enables them to enhance the hygroscopicity of aerosols, with potential climate impacts (Chan et al., 2011).

The formation pathways of organosulfates are complex and varied. They have been shown to be generated by non-homogeneous and multiphase reactions (Iinuma et al., 2007; Surratt et al., 2008). For example, Rudziński et al. (Rudziński et al., 2009) and Worton et al. (Worton et al., 2011) found that the photo-oxidation of a variety of biogenic volatile organic compounds, such as isoprene, α-pinene, and β-pinene, can lead to the formation of organosulfates. Noziere et al. suggested that the reaction products of sulfate anions with isoprene can yield organosulfates (Noziere et al., 2010; Nozière et al., 2015). Recent studies uncovered pathways by which organosulfates can be generated from the heterogeneous reaction of SO_2 with unsaturated bonds in fatty acids (Shang et al., 2016; Passananti et al., 2016). Organosulfates derived from organic acids were recently identified and characterized in fine particulate matter samples collected in the southeastern U.S., with glycolic acid sulfate being the most abundant (Hettiyadura et al., 2017).

Despite extensive research on the concentration, composition, and formation mechanisms of organosulfates, the limited knowledge of molecular-level mechanisms of their transformations hinders further understanding of their atmospheric processes as well as their physico-chemical properties (Huang et al., 2015). Organosulfates primarily exists in the particulate phase due to their low volatility (Estillore et al., 2016; George and Abbatt, 2010), although a non-negligible fraction has been shown to always be present in the gas-phase (Ehn et al., 2010; Le Breton et al., 2018) where they can react continuously with gas-phase oxidants (e.g., HO• radicals, O_3, and NO_3 radicals) at or near particle surfaces. The transformation of organosulfates generates not only new organic matter, but also inorganic sulfur species, such as HSO_4^- and SO_4^{2-}. Consequently, the conversion of organosulfates can significantly alter the composition and physico-chemical properties of atmospheric particulate matter (Hettiyadura et al., 2017). However, little is known in this regard. A few recorded studies include the chemical transformation of methyl sulfate, ethyl sulfate and an α-pinene-derived organosulfate by heterogeneous HO• oxidation (Kwong et al., 2018; Xu et al., 2022). Based on their observed reaction products, the authors suggested a mechanism proceeding through the formation of an alkoxy radical intermediate followed by fragmentation, yet the mechanism remains not fully elucidated. Moreover, organosulfates that can allow hydrogen abstraction at the β-position to the sulfate group could give rise to more complex mechanisms driven by Russell mechanism (Russell, 1957) and Bennett and Summers reaction (Bennett and Summers, 1974). While the presence of functional groups can exhibit specific features in the chemical transformation of organosulfates due to their complexity, their potential impact has not yet been thoroughly investigated.

Glycolic acid sulfate and methyl sulfate are two low molecular weight organic sulfates commonly found in the atmosphere, differing structurally by the α-substitution of a hydrogen atom by the carboxyl group. Both organosulfates have been detected

at various locations around the world at concentrations in the ranges 1.08×10^{6}-5.01×10^{7} molecule cm^{-3} for methyl sulfate (Hettiyadura et al., 2015; Peng et al., 2021) and 1.16×10^{7}-4.71×10^{8} molecule cm^{-3} for glycolic acid sulfate (Huang et al., 2018; Hettiyadura et al., 2015; Wang et al., 2021; Hughes and Stone, 2019; Cai et al., 2020; Liao et al., 2015). This study employs quantum chemical calculations to explore the transformation pathways of these organosulfates in both gas-phase and aqueous-phase environments, emphasizing the effects of carboxyl substitution. Ultimately, this study assesses the potential for sulfate formation and the atmospheric implications of these reactions.

2 Methods

2.1 Electronic structure calculations and thermochemistry

Quantum chemical calculations were used to investigate the transformation reactions of two organosulfates (methyl sulfate and glycolic acid sulfate), in the gas-phase and aqueous-phase. Geometry optimizations of all reaction states on the energy surface were performed with density functional theory using the Gaussian 09 package (Frisch et al., 2016). Pre-optimizations were first carried out using the M06-2X functional (Zhao and Truhlar, 2008) and the 6-31+G(d,p) basis set, and the best structures were further refined by the M06-2X/6-311+g(2df,2pd) method to yield the final structures. Vibrational frequency analysis on the M06-2X/6-311+g(2df,2pd) optimized structures were performed using the same method under the rigid rotor-harmonic oscillator approximation at 298.15 K and 1 atm at the same level of theory to yield zero-point energies and the thermochemical parameters. The continuum solvation model based on the solute electron density was used to model the aqueous-phase at the same level of theory as the gas-phase. This model is particularly suitable for describing atmospheric processes and effectively resolving the energy barriers (Ostovari et al., 2018; Xu and Coote, 2019; Cheng et al., 2019). In the aqueous-phase, the Gibbs free energies are calculated at standard temperature of 298.15 K and by converting the standard pressure of 1 atm (in the gas-phase) to the standard concentration of 1 M. Details are provided in Section S1 in the supplement. Single-point energy calculations on the M06-2X/6-311+g(2df,2pd) structures were performed with the CCSD(T)-F12/cc-pVDZ-F12 method using Orca version 4.2.1 (Riplinger and Neese, 2013). The M06-2X/6-311+g(2df,2pd) method has successfully been used in a series of previous studies (Ding et al., 2023; Wang et al., 2024; Cheng et al., 2022) and proved to efficiently resolve the transition state configuration. Given the size of the system investigated here, this level of theory appears to be a good compromise between accuracy and computation time.

2.2 Reaction kinetics

Reactions were modelled by assuming the pseudo-steady state approximation of the reactant complex formed from the interaction between initial reactants (organosulfate (OS = methyl sulfate or glycolic acid sulfate) and hydroxyl radical (HO•)). Based on this approximation, initial reactants are in equilibrium with the reactant complex that further rearranges through a transition state (TS) configuration to form the product complex according to the following reaction:

$$OS + HO\bullet \leftrightarrow \text{reactant complex} \rightarrow TS \rightarrow \text{product complex} . \quad (R1)$$

The reaction kinetics analysis was conducted by applying the transition state theory (Truhlar et al., 1996). Based on this theory applied to **reaction (R1)**, the biomolecular rate constant (k_{bim}) is given as

$$k_{bim} = K_{eq} k_{uni} , \quad (1)$$

where K_{eq} is the equilibrium constant of formation of the reactant complex, k_{uni} is the unimolecular rate constant of the transformation of the reactant complex to the product complex, respectively expressed by the following equations:

$$K_{eq} = \frac{1}{c^0} \times \exp\left(-\frac{\Delta G_{eq}}{RT}\right), \quad (2)$$

$$k_{uni} = \kappa \frac{k_B T}{h} \times \exp\left(-\frac{\Delta G^{\#}}{RT}\right). \quad (3)$$

In above equations, ΔG_{eq} is the Gibbs free energy of formation of the reactant complex from initial reactants, h is Planck's constant, k_B is Boltzmann's constant, $\Delta G^{\#}$ is the Gibbs free energy of the barrier separating the reactant complex from the product complex, R is the molar gas constant, T is the absolute temperature, and c^0 is the standard concentration (with values of 1 M and 2.46×10^{19} molecule cm^{-3} in the aqueous-phase and in the gas-phase, respectively, at 1 atm and 298.15 K). κ is the Eckart tunnelling coefficient (calculated by solving the Schrodinger equation for an asymmetrical one-dimensional Eckart potential (Eckart, 1930)).

While **Eq. (1)** is valid for calculating the biomolecular rate constants of gas-phase reactions, for aqueous-phase reactions, it is corrected by taking into account the contribution of the molecular diffusion described by the Collins-Kimball theory (Collins and Kimball, 1949). This leads to the overall rate constant for **reaction (R1)** in the aqueous-phase as follows

$$k_{overall} = \frac{k_{bim} \times k_D}{k_{bim} + k_D} . \quad (4)$$

k_D is the steady-state Smoluchowski rate constant calculated as (Smoluchowski M, 1917)

$$k_D = 4\pi R_{OS,HO} D N_A . \quad (5)$$

In **Eq. (5)**, $R_{OS,OH}$ stands for the reaction distance between the organosulfate and hydroxyl radical, defined as the sum of their respective radii, R_{OS} and R_{OH}. N_A is the Avogadro number and D is the sum of the diffusion coefficients of reactants (Truhlar, 1985). For a reactant i in water, the diffusion coefficient D_i is given by the Stokes-Einstein approach (Einstein, 1905) as follows:

$$D_i = \frac{k_B}{6\pi\eta R_i} . \quad (6)$$

The radii of reactants (organosulfate and hydroxyl radical), assumed to be spherical, were calculated by Eq. (6) using the Multiwfn software (Lu and Chen, 2012). All numerical values for radii, diffusion coefficients of reactants and the steady-state Smoluchowski rate constants are provided in **Tables S1** and **S2** in the Supplement.

3 Results and discussion

The reactions were explored both in the gas-phase and in aqueous-phase. A previous study indicated that, in the gas-phase, methyl sulfate and glycolic acid sulfate are likely to be hydrated under relevant atmospheric temperature and humidity (Tsona

and Du, 2019a). Hence, in this study the reactions with HO• in the gas-phase have been explored by considering methyl sulfate hydrates (CH_3-O-SO_3H···$(H_2O)_{n=0-2}$) and glycolic acid sulfate hydrates (HOOC-CH_2-O-SO_3H···$(H_2O)_{n=0-2}$).

3.1 Mechanism of methyl sulfate reaction with HO• radicals

3.1.1 CH_3-O-SO_3H···$(H_2O)_{0-2}$ + HO• reaction in the gas-phase

Our calculations indicate that CH_3-O-SO_3H···$(H_2O)_{n=0-2}$ reaction with HO• proceeds through formation of an intermediate reactant complex, HO•···CH_3-O-SO_3H···$(H_2O)_{n=0-2}$, in which the interaction between HO• and CH_3-O-SO_3H···$(H_2O)_{n=0-2}$ is mainly established through the hydrogen atom of HO• and one oxygen atom of CH_3-O-SO_3H. This intermediate reactant complex readily reacts through a hydrogen abstraction from the methyl group of CH_3-O-SO_3H by HO• to form the H_2C•-O-SO_3H···$(H_2O)_{n+1}$ product complex. A distinct feature was observed for n = 2, where the sulfate group was deprotonated, forming an ion pair with H_3O^+ (i.e, H_2C•-O-SO_3^-,H_3O^+···$(H_2O)_2$). This is likely because for this configuration, the minimum amount of water (2 molecules) necessary to achieve the stability of H_3O^+ in the gas-phase has been reached (Markovitch and Agmon, 2007; Heindel et al., 2018). Although the presence of water has a weak effect on the formation of the intermediate reactant complex, it substantially stabilizes the transition state towards the formation of the product complex by reducing the Gibbs free energy barrier from 6.45 kcal mol^{-1} for CH_3-O-SO_3H + HO• reaction to 3.52 kcal mol^{-1} for CH_3-O-SO_3H···$(H_2O)_2$ + HO• reaction. Energetics and structural details of this reaction are given in **Table 1** and **Figure 1**. The observed catalytic effect of water has been generally observed in some previous H-abstraction reactions (Wang et al., 2019; Wang et al., 2017; Zhang et al., 2024; Wang et al., 2024).

Unimolecular rate constants for the transformation of HO•···CH_3-O-SO_3H···$(H_2O)_n$ to H_2C•-O-SO_3H···$(H_2O)_{n+1}$ at 298 K were determined to be 1.15×10^{8} s^{-1}, 7.89×10^{7} s^{-1} and 1.59×10^{10} s^{-1}, corresponding to atmospheric lifetimes of 9 ns, 13 ns and 63 ps, for n = 0, 1, and 2, respectively, for the intermediate reactant complex. The lifetimes in the picosecond and nanosecond regimes indicate that HO•···CH_3-O-SO_3H···$(H_2O)_{n=0-2}$ complexes are indeed highly reactive and would most likely react fast before they could experience collisions with other abundant atmospheric oxidants (Bork et al., 2012). Hence, the immediate fate of HO•···CH_3-O-SO_3H···$(H_2O)_{n=0-2}$ is undoubtedly hydrogen abstraction by HO• to form H_2C•-O-SO_3H···$(H_2O)_{n+1}$. The bimolecular rate constant for this reaction is determined to be 1.14×10^{-13} cm^3 $molecule^{-1}$ s^{-1} at 298.15 K. As a radical, H_2C•-O-SO_3H···$(H_2O)_{n+1}$ would eventually undergo further decomposition depending on its stability, atmospheric lifetime and surrounding atmospheric conditions.

The stability of H_2C•-O-SO_3H···$(H_2O)_{n+1}$, examined relative to decomposition through the reverse reaction back to the HO•···CH_3-O-SO_3H···$(H_2O)_n$ complex, reveals barriers heights of 28.64, 24.92 and 24.55 kcal mol^{-1} for n = 0, 1, and 2, corresponding to unimolecular rate constants of 6.16×10^{-9} s^{-1}, 3.30×10^{-6} s^{-1} and 6.14×10^{-6} s^{-1}, respectively. These low-rate constants indicate that once formed, H_2C•-O-SO_3H···$(H_2O)_{n+1}$ would not react back to form initial reactants before possible collision with atmospheric oxidants have occurred. Beside hypothesizing self-decomposition to be a likely outcome of H_2C•-O-SO_3H, observed atmospheric lifetimes indicate that its fate would depend upon collisions with most atmospheric oxidants,

including O_2, O_3 and NO_2. Considering that water is known to evaporate fast from atmospheric species, H_2C•-O-SO_3H would readily react both in its unhydrated and its hydrated forms.

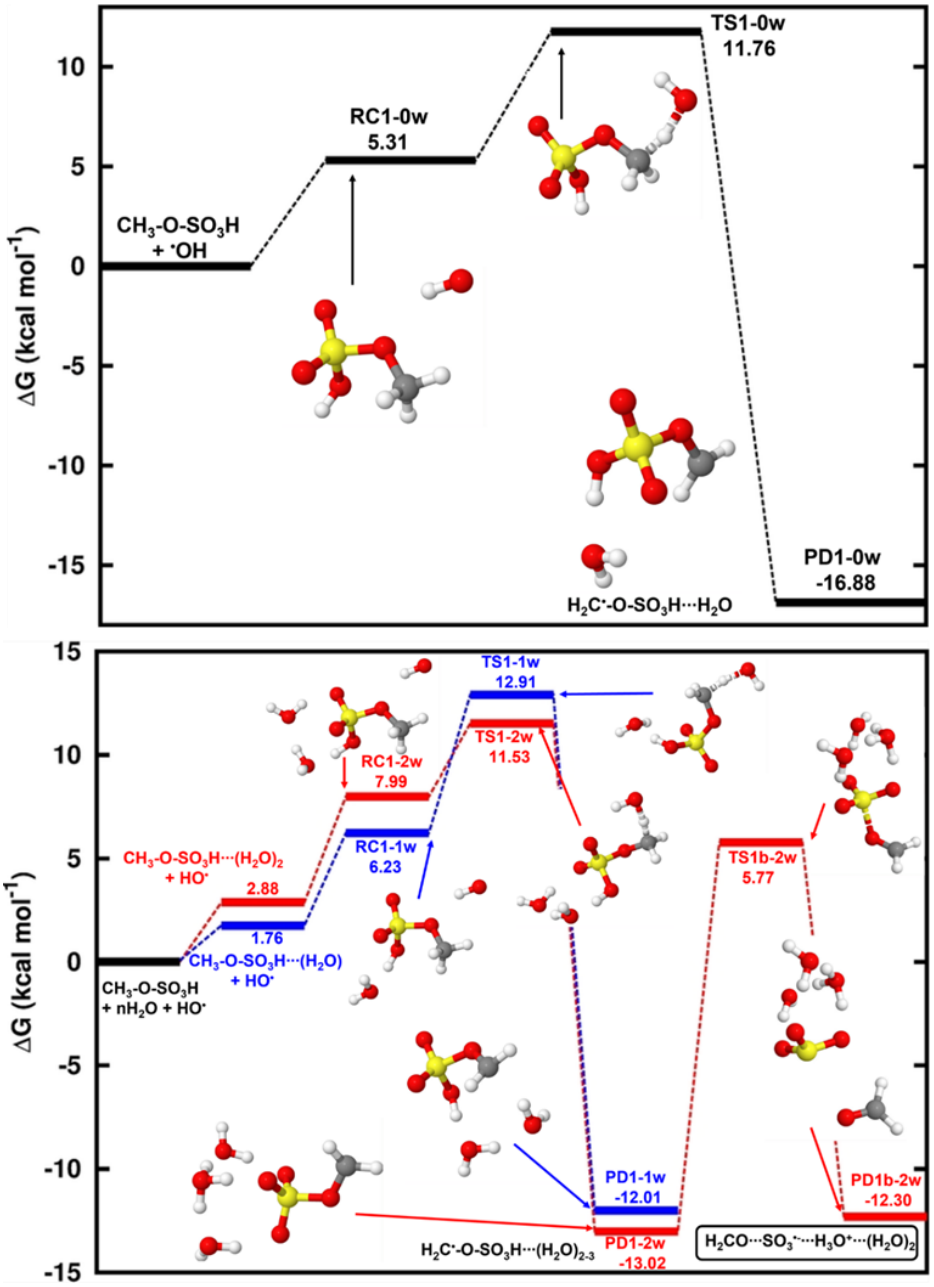

Figure 1: Gibbs free energy changes (in kcal mol^{-1}) and optimized structures for all intermediates in the reaction of CH_3-O-SO_3H···$(H_2O)_{n=0-2}$ with HO• radicals. The top panel is the reaction in the absence of water and the bottom panel is the reaction in the presence of water, where the blue indicates the monohydrated reaction and the red line indicates the dihydrated reaction. The sulfur atom is yellow, the oxygen atom is red, the carbon atom is grey and the hydrogen atom is white.

Based on these observations, the fate of H_2C•-O-SO_3H was examined relative to the following decomposition processes:

H_2C•-O-$SO_3H\cdots(H_2O)_n \rightarrow H_2CO + SO_3$•$^-$,$H_3O^+\cdots(H_2O)_{n-1}$, (R2)

H_2C•-O-$SO_3H\cdots(H_2O)_n + NO_2 \rightarrow ON + H_2CO + SO_4$•$^-\cdots H_3O^+\cdots(H_2O)_{n-1}$, (R3)

H_2C•-O-$SO_3H\cdots(H_2O)_n + O_3 \rightarrow O_2 + HCO$• + H_2SO_4 + (n-1)H_2O , (R4)

H_2C•-O-$SO_3H + O_2 \rightarrow \rightarrow HC(O)$-O-$SO_3H$. (R5)

Our attempts to optimize the self-decomposition of H_2C•-O-$SO_3H\cdots(H_2O)_n$ failed but for n = 3 (**reaction (R2)**). This was as expected since the gas-phase stability of H_3O^+ can only be achieved by solvation with at least two water molecules (Markovitch and Agmon, 2007; Heindel et al., 2018).

Reaction (R2) proceeds by one S-O bond breaking and a hydrogen transfer from -SO_3H to H_2O to release the $H_2CO\cdots SO_3$•$^-$,$H_3O^+\cdots(H_2O)_2$ complex. The transition state in this process was located at 18.79 kcal mol^{-1} above $H_2C^{\bullet}$-O-SO_3^-,$H_3O^+\cdots(H_2O)_2$. To confirm the location of the free electron on the different states of H_2C•-O-$SO_3H\cdots(H_2O)_3$ decomposition, the analysis of the charge distribution was performed. As shown in **Figure 2(A)**, the electronic charge initially located on the CH_2- fragment progressively migrates through along the H_2C•-O-SO_3H core to ultimately rest on SO_3, leaving CH_2O electronically neutral. Although SO_3•$^-$ and H_2CO are expected products of this decomposition, our calculations show that the outcome of this reaction can only be moderate due to the relatively high energy barrier. Several experimental and theoretical studies showed that $SO_3^{\bullet-}$ would quickly hydrate in the gas-phase to form $SO_3^{\bullet-}\cdots(H_2O)_n$ cluster wherein the oxidation to sulfuric acid occurs in a mechanism stabilized and catalyzed by a free electron (Bork et al., 2013; Tsona and Du, 2019b; Fehsenfeld and Ferguson, 1974; Svensmark et al., 2007; Enghoff and Svensmark, 2008). Considering this outcome for $SO_3^{\bullet-}$ in the gas-phase, H_2CO and inorganic sulfate are expected products of the gas-phase reaction of methyl sulfate with HO• at ambient conditions. The calculated unimolecular rate constant of this decomposition at 298.15 K, 1.03×10^{-1} s^{-1}, indicates that this process can account for the fate of H_2C•-O-SO_3H only under the conditions of low oxidants. The products predicted by our calculations were observed in a previous experimental study by Kwong et al. (Kwong et al., 2018) for the same reaction, and the mechanisms from Russell (Russell, 1957) and Bennett and Summers (Bennett and Summers, 1974) were speculated by the authors to explain this formation. Besides these mechanisms, **reaction (R2)** in this study might be a complementary mechanism to the formation of inorganic sulfate and formaldehyde from the reaction of methyl sulfate with HO•, at least at a certain degree of hydration or humidity.

Besides the self-decomposition of H_2C•-O-SO_3H, we further examined its reactions with NO_2 (**reaction (R3)**), O_3 (**reaction (R4)**), and O_2 (**reaction (R5)**). We found that for **reaction (R3)**, SO_4•$^-$ + H_2CO + NO formation would be prevented by a high Gibbs free energy barrier (~74 kcal mol^{-1}), regardless of the number of water molecules involved. Energetics of this reaction are given in **Table S3** and **Figure S1**. This high energy barrier is likely related to the difficulty in breaking the ON-O and C-O bonds to release the products. We conclude that **reaction (R3)** is likely without atmospheric significance to the chemistry of CH_3-O-SO_3H under relevant atmospheric conditions.

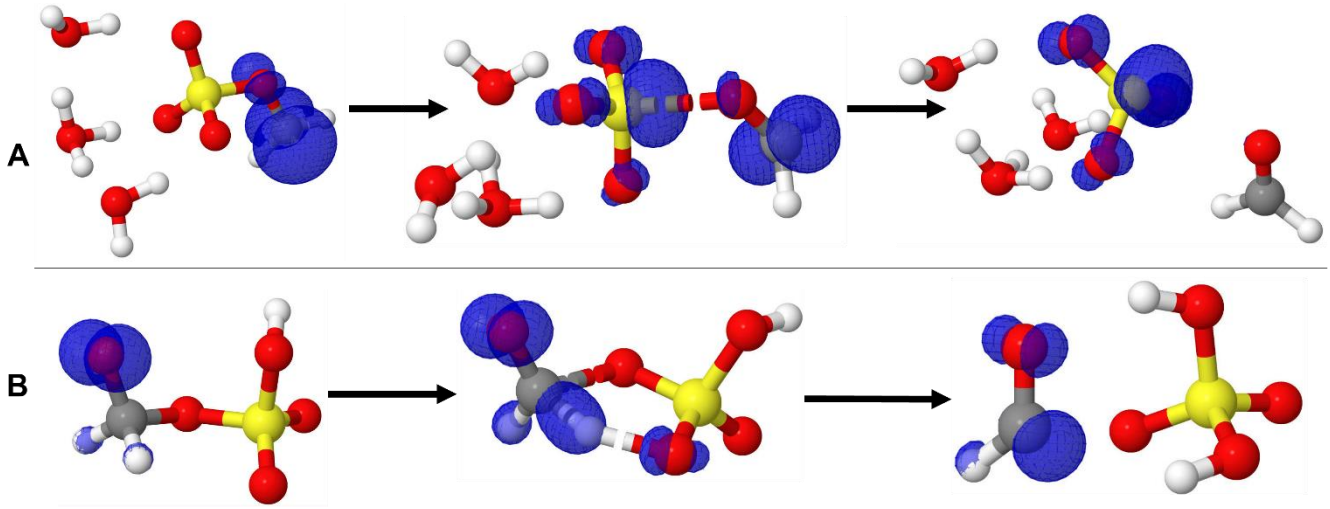

Figure 2: Representation of the spin density (blue color) on the electronic states of the decomposition of (A) H_2C•-O-SO_3H···$(H_2O)_3$, and (B) •O-H_2C-O-SO_3H. From left to right are the reactant, transition state and the product complex, respectively. The sulfur atom is yellow, the oxygen atom is red, the carbon atom is grey and the hydrogen atom is white.

The reaction of H_2C•-O-SO_3H···$(H_2O)_n$ with O_3 was examined thereafter. Regardless of the presence or the absence of water, this reaction proceeds through a submerged energy barrier, with the general mechanism following two main steps: the interaction of H_2C•-O-SO_3H with O_3 and the unimolecular decomposition of the resulting intermediate product. The interaction of H_2C•-O-SO_3H···$(H_2O)_n$ with O_3 led to exergonic formation of the O_3···H_2C•-O-SO_3H···$(H_2O)_n$ intermediate reactant complex. The formed reactant complexes are further transformed through an oxygen transfer from O_3 to H_2C•-O-SO_3H···$(H_2O)_n$ via transition state configurations to form alkoxyl radicals •O-CH_2-O-SO_3H···$(H_2O)_n$. The energy barrier in this transformation in the absence of water is located 7.02 kcal mol^{-1} below corresponding reactant complex and is weakly altered by the presence of water. The exergonic formation of O_3···H_2C•-O-SO_3H···$(H_2O)_n$ and the submerged barrier in its transformation are indicative of instantaneous formation of •O-CH_2-O-SO_3H···$(H_2O)_n$ from H_2C•-O-SO_3H···$(H_2O)_n$ with O_3.

Table 1: Electronic energy changes (ΔE) and Gibbs free energy changes (ΔG at 298.15 K and 1 atm) for all intermediate species in the reaction of methyl sulfate with HO• radicals. Energy units are kcal mol^{-1}. "RC" stands for intermediate reactant complex, "TS" stands for transition state, "PD" stands for product, "nw" stands for the number of added water molecules to the reaction of methyl sulfate with HO• radicals.

Reaction	ΔG	ΔE
CH_3-O-SO_3H···$(H_2O)_{n=0-2}$ + •OH ↔ RC1-nw → TS1-nw → PD1-nw (H_2C•-O-SO_3H···$(H_2O)_{n+1}$)		
	n = 0	
RC1-0w	5.31	-2.57
TS1-0w	11.76	5.66
PD1-0w	-16.88	-26.17
	n = 1	

RC1-1w	6.23	-13.38
TS1-1w	12.91	-5.16
PD1-1w	-12.01	-32.34
	n = 2	
RC1-2w	7.99	-22.64
TS1-2w	11.53	-18.10
PD1-2w	-13.02	-46.65

H_2C•-O-SO_3^-,H_3O^+···$(H_2O)_2$ → TS1b-2w → PD1b-2w (H_2CO···SO_3•$^-$,H_3O^+···$(H_2O)_2$)		
H_2C•-O-SO_3^-,H_3O^+···$(H_2O)_2$	0	0
TS1b-2w	18.79	23.35
PD1b-2w	0.72	7.09

H_2C•-O-SO_3H + O_3 ↔ RC31→ TS31 → PD31 (O_2 + •O-CH_2-O-SO_3H) → RC31b → TS31b → PD31b		
RC31	-18.70	-37.32
TS31	-25.72	-42.17
PD31	-22.48	-34.73
RC31b	-4.48	5.22
TS31b	10.42	26.55
PD31b	-22.24	-7.05

H_2C•-O-SO_3H + O_2 → •OO-CH_2-O-SO_3H	-45.98	-65.69

•OO-CH_2-O-SO_3H + •OO-CH_2-O-SO_3H → RC32 → TS32 → PD32		
RC32	-99.39	6.28
TS32	-83.49	15.33
PD32	-234.34	-10.68

Optimized structures and energetics of all reactions states in these reactions are given in **Figure 3**, **Figure S2**, **Table 1** and **Table S4**. The direct product of this transformation is a sulfonate alkoxy radical, •O-H_2C-O-SO_3H, which further decomposes through the C-O bond cleavage and hydrogen transfer from •O-CH_2- to -SO_3H to form the H_2SO_4···HCO• product complex with substantial energy gain. The electronic charge distribution on •O-H_2C-O-SO_3H in the reactant and on $HCO^{\bullet}$ in the product complex was confirmed by our electronic charge analysis as shown in **Figure 2(B) and Figure S3**. The barrier height to this

decomposition is significantly lowered from 14.90 kcal mol^{-1} (for H_2C•-O-SO_3H) to 6.59 kcal mol^{-1} (for H_2C•-O-$SO_3H\cdots(H_2O)_3$). These correspond respectively to unimolecular rate constants of 7.38×10^{1} s^{-1} and 9.06×10^{7} s^{-1} at 298.15 K. The particular stability of the transition state in H_2C•-O-$SO_3H\cdots(H_2O)_3$ decomposition can be attributed to the mediation of the additional water molecule in the hydrogen transfer from •O-CH_2- to -SO_3H. This is in line with the demonstrated increasing catalytic role of water with increasing number of water molecules in SO_3 hydrolysis to sulfuric acid (Larson et al., 2000; Hofmann and Schleyer, 1994; Hofmann-Sievert and Castleman, 1984; Morokuma and Muguruma, 1994; Loerting and Liedl, 2000). The currently presented mechanism for $H_2SO_4\cdots$HCO• formation from C-O bond cleavage was suggested by Huang et al. (Huang et al., 2018) to explain bisulfate formation from the fragmentation of organosulfates. Compared to H_2C•-O-SO_3H self-decomposition and reaction with NO_2, the reaction with O_3 is the most energetically and kinetically favorable process. Nonetheless, considering all the processes by **reactions (R2)-(R4)**, it is obvious that the main products of the gas-phase reaction of methyl sulfate with HO• are formaldehyde (H_2CO) and sulfuric acid (H_2SO_4). This agrees with the experimental observation by Kwong et al. (Kwong et al., 2018).

Contrary to the self-decomposition of H_2C•-O-SO_3H and reactions with NO_2 and O_3 that are favorable with H_2C•-O-SO_3H hydrates, we were unable to fully optimize the O_2 reaction with H_2C•-O-SO_3H hydrates but with the unhydrated system, instead. This led to exergonic formation of the •OO-CH_2-O-SO_3H peroxyl radical with 45.98 kcal mol^{-1} Gibbs free energy gain. The chemistry of peroxyl radicals has been the subject of several experimental and theoretical studies. It is widely accepted that the peroxyl radical would predominantly decompose to form alkoxyl radicals or alcohols along with carbonyl compounds through tetroxide intermediates (Russell, 1957). However, although the end products from this decomposition have been verified experimentally, the mechanisms have often been deemed unlikely due to inconsistency between thermodynamic experiments and computational studies (Nangia and Benson, 1980; Zhang et al., 2012; Liang et al., 2011). Moreover, the effort to elucidate alcohols and carbonyl compounds formation from the decomposition of the tetroxide in a previous study could not be achieved due to the impossibility to determine the corresponding transition states (Ghigo et al., 2003), while alkoxyl radical formation was observed to simply correspond to the dissociation of the tetroxide. A most recent theoretical study specifically focusing on the decomposition pathways of the tetroxide intermediate indicated that although substantial uncertainties may exist in their computed energetics, alkoxyl radicals are likely primary products from atmospherically relevant peroxyl radicals (Salo et al., 2022). Following the above reasoning, our calculations indicate that two molecules of •OO-CH_2-O-SO_3H recombine to form a tetroxide that can further decompose to generate two alkoxyl radicals •O-CH_2-O-SO_3H clustered to molecular oxygen. Then, the two •O-CH_2-O-SO_3H radicals quickly interact with O_2 to form H_2O_2 and formic sulfuric anhydride (HC(O)-O-SO_3H) (**reaction (R5)**). The latter product has been identified to enhance new particle formation (An, 2024). Energetics and structures of all intermediates in this reaction are given in **Figure 3**.

Considering the recombination of two H_2C•-O-SO_3H molecules as another likely fate of H_2C•-O-SO_3H the absence of other reaction partners such as O_2, O_3, or NO_2 besides self-decay, our preliminary calculations indicate that this recombination would occur fast and would proceed through C-C bond formation via a barrierless process. However, the relevance of the resulting

product is not clearly established and its fate may mostly depend on reactions initiated by a hydrogen abstraction from the -CH_2- group.

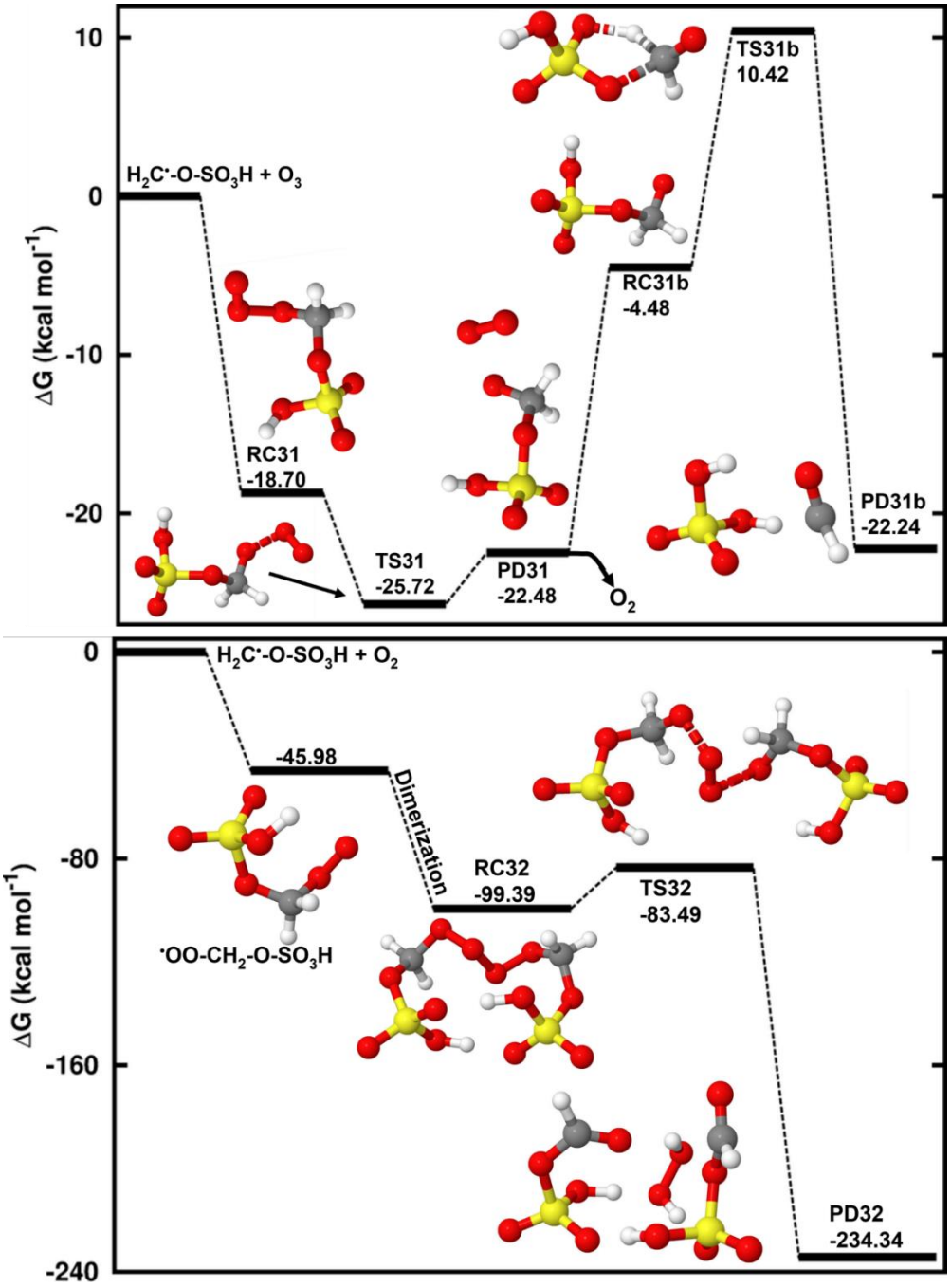

Figure 3: Gibbs free energy changes (in kcal mol^{-1}) and optimized structures for all intermediates in the reaction of H_2C•-O-SO_3H with O_3 (top) and O_2 (bottom). The sulfur atom is yellow, the oxygen atom is red, the carbon atom is grey and the hydrogen atom is white.

The studied reaction of methyl sulfate with HO• radicals in the gas-phase shows an example of the main processes through which organosulfates may be converted into inorganic sulfates. Humidity is seen to play a non-negligible role in the effective reaction of methyl sulfate while from the kinetics point of view, O_3 is a key oxidant besides O_2 in the intermediate steps.

3.1.2 CH_3-O-SO_3^- + HO• reaction in the aqueous-phase

In the aqueous-phase, methyl sulfate (CH_3-O-SO_3^-) undergoes similar steps as its electronically neutral counterpart to form the product complex, H_2C•-O-SO_3^-···H_2O. **Figure 4** shows the Gibbs free energy surface for this reaction at 298.15 K and 1 M concentration, along with the structures of all stationary states. Further energetics details for this reaction are given in **Table 2**. We determined a Gibbs free energy barrier of 3.54 kcal mol^{-1} for this reaction (4.69 kcal mol^{-1} lower than in the CH_3-O-SO_3H + HO• reaction), and a bimolecular rate constant of 7.87×10^6 M^{-1} s^{-1}. This value is about 13 times lower than a previous experimental value (Gweme and Styler, 2024), and the difference can be attributed both to computational errors and environmental factors. The formation of H_2C•-O-SO_3^-···H_2O occurred with substantial Gibbs free energy gain, -14.28 kcal mol^{-1}, stable enough towards decomposition to initial reactants for which the energy barrier 23.89 kcal mol^{-1} is found (see **Figure 4**). Based on this energy barrier height, we determined an atmospheric lifetime of 0.61 days for H_2C•-O-SO_3^-···H_2O. This indicates that besides self-decomposition as an alternative chemical fate, H_2C•-O-SO_3^-···H_2O will live long enough to experience collisions with abundant atmospheric oxidants. While NO_2 dissolves effectively in water and is known to react with molecular water to produce nitric acid which is highly soluble in water (Ford and Miranda, 2020; Tan and Piri, 2013; Lee and Schwartz, 1981; England and Corcoran, 1974), the stability of O_3 solubility in water is readily affected by various factors including ozone concentration, pH and ultraviolet light (Lovato et al., 2009). Depending on environmental conditions, ozone can react via a direct reaction pathway involving molecular ozone or by an indirect route involving reactive intermediates that arise from its decomposition (Buehler et al., 1984; Buhler et al., 1984; Staehelin et al., 1984; Staehelin and Hoigne, 1982). Moreover, O_3 is known to be 13 times more soluble in water than O_2 (Seinfeld and Pandis, 1998). Hence, besides the self-decay reaction, the fate of H_2C•-O-SO_3^- was examined via reactions with O_2 and O_3:

H_2C•-O-SO_3^- → H_2CO + SO_3•$^-$, (R6)

H_2C•-O-SO_3^- + O_3 → O_2 + HSO_4^- + HCO• , (R7)

H_2C•-O-SO_3^- + O_2 → → HSO_4^- + HCO• . (R8)

While inspecting the vibrational modes of H_2C•-O-SO_3^-, it is obvious that dissociation along the H_2C•O-SO_3 bond to form H_2CO + SO_3•$^-$ (**reaction (R6)**) would be a possible chemical fate. The analysis of electronic charge distribution on H_2C•-O-SO_3^- confirms that the unpaired electron initially on CH_2- gradually migrates to completely rest on SO_3 in the products, leaving CH_2O uncharged (see **Figure S4**). This process was examined and a Gibbs free energy barrier height of 18.90 kcal mol^{-1} was found (see **Figure 4**), which corresponds to a unimolecular rate constant of 8.56×10^{-2} s^{-1} at 298.15 K. This is nearly equal to the rate constant of the similar step (1.03×10^{-1} s^{-1}) in the reaction of CH_3-O-SO_3H under humid conditions. The predicted relatively low-rate constant of H_2C•-O-SO_3^- decomposition to H_2CO and SO_3•$^-$ can only account for CH_3-O-SO_3^- fate under the conditions of low oxidants concentrations.

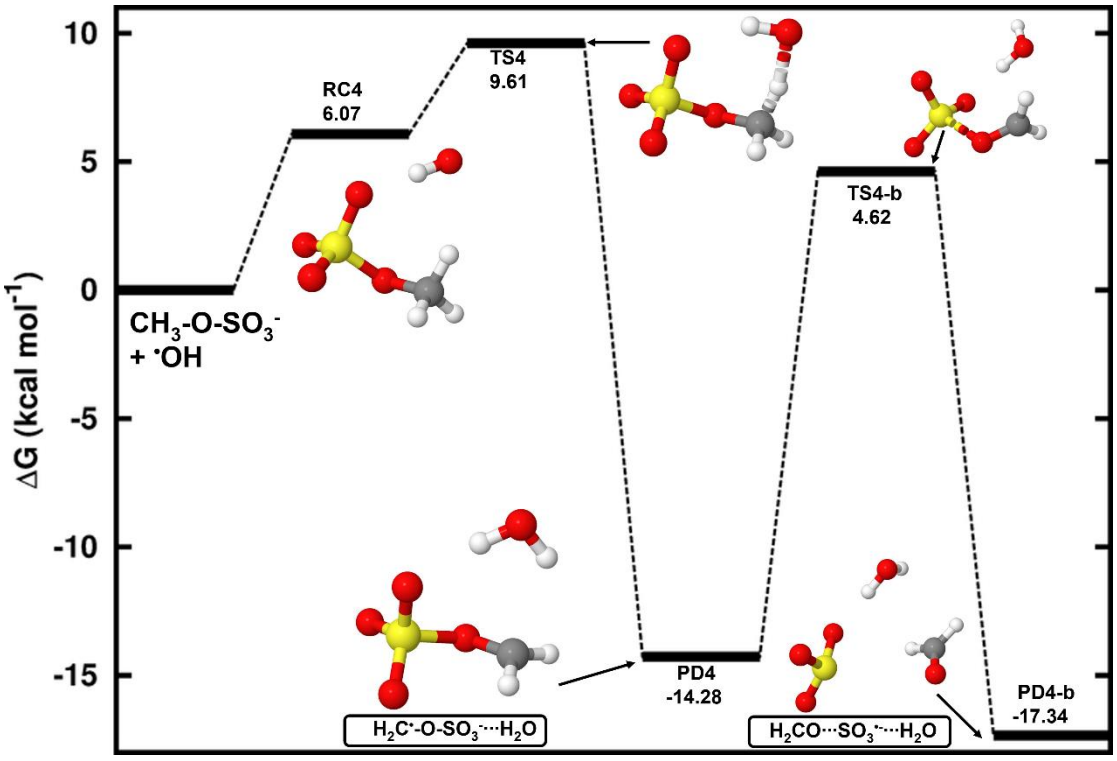

Figure 4: Gibbs free energy changes (in kcal mol^{-1}) and optimized structures for all intermediates in the reaction of CH_3-O-SO_3^- with HO• radicals. The sulfur atom is yellow, the oxygen atom is red, the carbon atom is grey and the hydrogen atom is white.

Table 2: Gibbs free energy changes (ΔG) for all intermediate species in the reaction of deprotonated methyl sulfate with HO• radicals at 298.15 K and 1 M. Energy units are kcal mol^{-1}. "RC" stands for intermediate reactant complex, "TS" stands for transition state and "PD" stands for product.

Species	**ΔG**
CH_3-O-SO_3^- + •OH ↔ RC4 → TS4 → PD4 (H_2C•-O-SO_3^-···H_2O) H_2C•-O-SO_3^-···H_2O → TS4-b → PD4-b (H_2CO···SO_3•-···H_2O)	
RC4	6.07
TS4	9.61
PD4	-14.28
TS4-b	4.62
PD4-b	-17.34
H_2C•-O-SO_3^- + O_3 ↔ RC5 → TS5 → PD5 (•O-H_2C-O-SO_3^- + O_2) •O-H_2C-O-SO_3^- (RC5-b) → TS5-b → PD5-b (HSO_4^-···HCO•)	

RC5	-52.05
TS5	-58.03
PD5	-59.64
RC5-b	-44.72
TS5-b	-36.80
PD5-b	-60.73
H_2C•-O-SO_3^- + O_2 → •OO-CH_2-O-SO_3^- (PD6)	-54.83
•OO-CH_2-O-SO_3^- + •OO-CH_2-O-SO_3^- ↔ RC7 → TS7 → PD7 → •O-CH_2-O-SO_3^-	
RC7	-103.58
TS7	-89.46
PD7	-141.39
HOOC-CH_2-O-SO_3^- + •OH ↔ RC8 → TS8 → PD8 (HOOC-CH•-O-SO_3^-···H_2O) HOOC-CH•-O-SO_3^- (RC9) → TS9 → PD9 (HOOC-CHO··· SO_3•$^-$)	
RC8	5.61
TS8	11.52
PD8	-18.08
RC9	-5.69
TS9	12.98
PD9	-3.66
HOOC-CH•-O-SO_3^- + O_3 → O_2 + HOOC-CH(O)•-O-SO_3^-	-47.79
HOOC-CH•-O-SO_3^- + O_2 → HOOC-CH(OO)•-O-SO_3^-	-43.01

Considering H_2C•-O-SO_3^- interaction with O_3 (**reaction (R7)**), this reaction is completely downhill, and it follows two main steps: formation of an alkoxy radical and decomposition of the latter into HSO_4^- and HCO• radical (see **Figure 5**). The first step is highly exergonic, with the reactant complex (O_3···H_2C•-O-SO_3^-) being formed with -52.05 kcal mol^{-1} Gibbs free energy change. The decomposition of O_3···H_2C•-O-SO_3^- into O_2···•O-H_2C-O-SO_3^- product complex is almost instantaneous, with the Gibbs free energy barrier located 5.98 kcal mol^{-1} below the reactant. As O_2 evaporates from the product complex, the resulting alkoxy radical, •O-H_2C-O-SO_3^-, is rapidly decomposed to HSO_4^- and HCO•, by overcoming a relatively low energy barrier

(7.92 kcal mol^{-1}). The charge analysis confirms that during •O-H_2C-O-SO_3^- decomposition, the unpaired electron effectively delocalizes from the oxygen atom of the alkoxy functional group to concentrate on the carbon atom of HCO (see **Figure S4**), leaving HSO_4^- as one of the main products. These products were also identified as primary products in CH_3-O-SO_3^- reaction with •OH, although a different formation mechanism was proposed (Kwong et al., 2018). This study demonstrates that the reaction with O_3 is distinctly thermodynamically and kinetically favorable, therefore highlighting the presented mechanism to be a determinant step in the oxidation of methyl sulfate by •OH radicals. While the role of HSO_4^- in the atmosphere is clearly established, for example in aerosol formation, HCO• has never been observed in aqueous media. Its presence has only been revealed through indirect observations and it is suggested to react fast with surrounding water to form formaldehyde (Jensen et al., 2010).

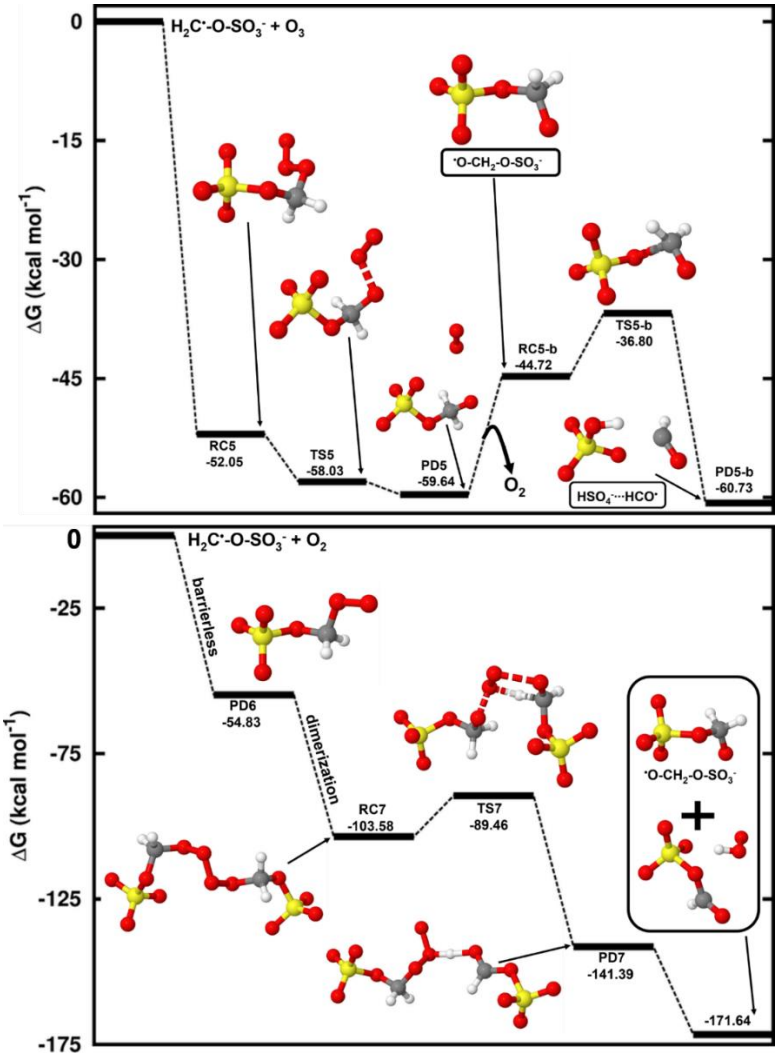

Figure 5: Gibbs free energy changes (in kcal mol^{-1}) and optimized structures for all intermediates in the reaction of CH_2•-O-SO_3^- with O_3 (top panel) and O_2 (low panel). The sulfur atom is yellow, the oxygen atom is red, the carbon atom is grey and the hydrogen atom is white.

H_2C•-O-SO_3^- can also react fast with O_2 (**reaction (R8)**) to form a peroxyl radical (•OO-CH_2-O-SO_3^-) through a barrierless process with the release of 54.83 kcal mol^{-1} Gibbs free energy. Based on the above on the chemistry of peroxyl radicals, two molecules of •OO-CH_2-O-SO_3^- can combine to form a tetroxide, which can further decompose to generate •O-CH_2-O-SO_3^- by overcoming a Gibbs free energy barrier of 14.12 kcal mol^{-1} (see **Figure 5**). The alkoxy radical •O-CH_2-O-SO_3^- can readily decompose to form HSO_4^- and HCO•, by overcoming a barrier of 7.92 kcal mol^{-1} and as explained above and exemplified in **Figure 5**, its formation from H_2C•-O-SO_3^- reaction with O_2 is less thermodynamically favorable than with O_3, despite the overall rate of the former can be higher than that of the latter due to the high concentration of O_2. It follows from the above mechanisms that in most atmospherically relevant conditions, the pathway for •O-CH_2-O-SO_3^- formation from H_2C•-O-SO_3^- reaction with O_3 can readily complement that from Bennett and Summers that involves reaction with O_2 (Bennett and Summers, 1974).

In addition to the mechanisms speculated by experimental studies (Kwong et al., 2018), the combination of mechanisms both in the gas-phase and in aqueous-phase presented in this study provides additional pathways for inorganic sulfate formation from the reaction of methyl sulfate with HO• radicals, namely the decomposition of H_2C•-O-SO_3^- or H_2C•-O-SO_3H and their reactions with O_3. These processes can drive significant changes in the chemical composition of aerosol, especially in terms of sulfate mass loadings.

3.2 Reaction mechanism of glycolic acid sulfate with HO• radicals

Hydrogen abstraction from glycolic acid sulfate could occur both from -CH_2- and -COOH groups according to the following reactions:

HOOC-CH_2-O-SO_3H + HO• → H_2O + HOOC-CH•-O-SO_3H , (R9)

HOOC-CH_2-O-SO_3H + HO• → H_2O + •OC(O)-CH_2-O-SO_3H . (R10)

The mechanism of **reaction (R9)** is similar to that of the hydrogen abstraction from methyl sulfate that forms an alkyl radical. Through this process, glycolic acid sulfate readily undergoes a hydrogen abstraction from the -CH_2- group by HO•, resulting in HOOC-CH•-O-SO_3H formation. The reactant complex in this process lies at 4.65 kcal mol^{-1} at 298.15 K and 1 atm, and the transition state for its conversion is located 2.13 kcal mol^{-1} above the reactant complex. We determined a bimolecular rate constant of the overall reaction is 6.17 $\times 10^{-12}$ cm^3 $molecule^{-1}$ s^{-1} for this reaction at 298.15 K. This shows that hydrogen abstraction by •OH from glycolic acid sulfate is more favorable than from methyl sulfate, hereby highlighting the enhancing effect of the carboxyl substituent. The further chemistry of HOOC-CH•-O-SO_3H is examined through reactions with O_3 and O_2. Our calculations show that contrary to the reaction with H_2C•-O-SO_3H, O_3 hardly reacts with HOOC-CH•-O-SO_3H as the O_3···HOOC-CH•-O-SO_3H formation is highly endergonic at standard conditions. However, the reaction with O_2 is seen to be fast, proceeding through formation of the reactant complex that is readily converted to HOOC-CH(OO)•-O-SO_3H. The observed negative Gibbs free energy barrier (-9.02 kcal mol^{-1} below the reactant complex) in this conversion indicates that the formation of HOOC-CH(OO)•-O-SO_3H is almost instantaneous at standard conditions. Two molecules of HOOC-CH(OO)•-

355 O-SO_3H develop into a tetroxide that then decomposes to HC(O)-O-SO_3H and HOOC-CH(O)•-O-SO_3H. The energetics of this reaction are provided in **Figure 6** and **Table S5**.

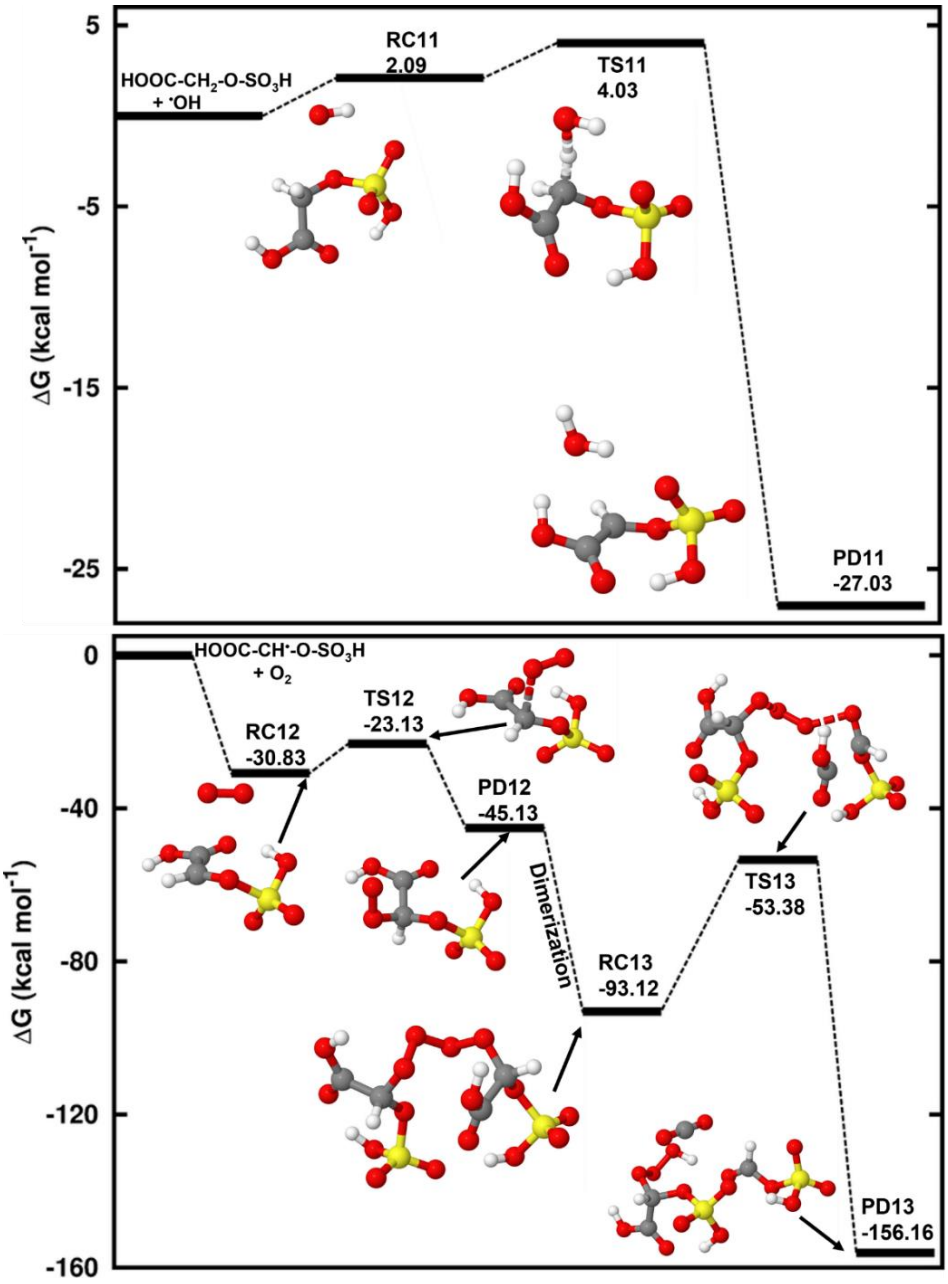

Figure 6: Gibbs free energy changes (in kcal mol^{-1}) and optimized structures for all intermediates in the reaction of HOOC-CH_2-O-
360 **SO_3H reaction with HO• radicals proceeding through hydrogen abstraction from the -CH_2- group (top) and in the HOOC-CH•-O-SO_3H reaction with O_2 (bottom). The sulfur atom is yellow, the oxygen atom is red, the carbon atom is grey and the hydrogen atom is white.**

The abstraction from -COOH led to •OC(O)-CH_2-O-SO_3H (**reaction (R10)**) that further decomposes to methylene sulfate radical (H2C•-O-SO3H) and CO2. The structures and energetics of all intermediate states of this reaction are given in **Figure S5** and **Table S6** in the Supplement. At the same level of theory, we determined a biomolecular rate constant of 3.86 $\times 10^{-14}$ cm^3 $molecule^{-1}$ s^{-1}, two orders of magnitude lower than the hydrogen abstraction from the -CH_2- group. This indicates that hydrogen abstraction from glycolic acid would follow two competitive pathways although the pathway leading the alkyl radical would be somewhat preferred. It can be inferred that for organosulfates that have a -COOH substituent at the β-position relative to the sulfate group, decarboxylation would be a possible outcome of their decomposition. The chemistry of H_2C•-O-SO_3H was assessed in Section 3.1 above.

We further investigated the HO•-initiated reaction of glycolic acid sulfate in the aqueous-phase, where the deprotonated state, HOOC-CH_2-O-SO_3^-, is predominant. The preliminary interaction in this reaction is similar to that in the reaction of CH_3-O-SO_3^-, with HO• abstracting the hydrogen atom from the -CH_2- group to form the product complex, HOOC-CH•-O-$SO_3^-\cdots H_2O$. The energies and structures of all different stationary states of this reaction are given in **Figure 7**, while further energetics details are provided in **Table 2**. A bimolecular rate constant of 7.29×10^8 $M^{-1}s^{-1}$ is determined for this reaction, in good agreement with the experimental report by Buxton et al. (Buxton et al., 1988). HOOC-CH•-O-$SO_3^-\cdots H_2O$ formation is highly exergonic, with -18.69 kcal mol^{-1} Gibbs free energy at 298.15 K and 1 M. Its decomposition back to initial reactants is prevented by a substantially high energy barrier of 29.60 kcal mol^{-1}. Based on this backward process, an atmospheric lifetime of 6.30×10^8 s^{-1} is predicted for HOOC-CH•-O-$SO_3^-\cdots H_2O$ under relevant atmospheric conditions, long enough for this product complex to be subject to collisions with nearly all relevant atmospheric oxidants. H_2O further dissociates from the product complex, leaving bare HOOC-CH•-O-SO_3^- to undergo the following decomposition processes:

HOOC-CH•-O-SO_3^- → HOOC-CHO + $SO_3^{\bullet-}$, (R9)

HOOC-CH•-O-SO_3^- + O_3 → O_2 + HOOC-CH$^{\bullet}$(O)-O-SO_3^- , (R10)

HOOC-CH•-O-SO_3^- + O_2 → → HOOC-CH$^{\bullet}$(O)-O-SO_3^- . (R11)

Following **reaction (R9)**, HOOC-CH•-O-SO_3^- can undergo O-SO_3 bond cleavage and form the HOOC-CHO$\cdots SO_3^{\bullet-}$ product complex at a unimolecular rate constant of 1.24×10^{-1} s^{-1}. The electronic charge analysis (shown in **Figure S6(A)**) confirms the distribution of the unpaired electron on SO_3 while HOOC-CHO is electrically neutral. Knowing that $SO_3^{\bullet-}$ has no other atmospheric chemical fate than inorganic sulfate, it follows that glycolic acid sulfate transformation by HO•-initiated reaction would produce glyoxylic acid and sulfate at a nearly equal rate constant as CH_2•-O-SO_3^- for a similar mechanism. The significance of this reaction will, however, depend on the rates of HOOC-CH•-O-SO_3^- reactions via other pathways.

Similar to H_2C•-O-SO_3^-, HOOC-CH•-O-SO_3^- reaction with O_3 is completely downhill and directly undergoes an oxygen atom transfer for O_3 to the -CH- group, forming the alkoxy radical, HOOC-CH(O)•-O-SO_3^- (**reaction (R10)**). HOOC-CH(O)•-O-SO_3^- is susceptible to further decompose to CO_2 + HCO• + HSO_4^-. However, we were unable to locate the appropriate transition state, which is seemingly associated with the mesomeric effect induced by the presence of an unpaired electron and entertained by the -COOH function. This situation was not observed in the decomposition of •O-CH_2-O-SO_3^-.

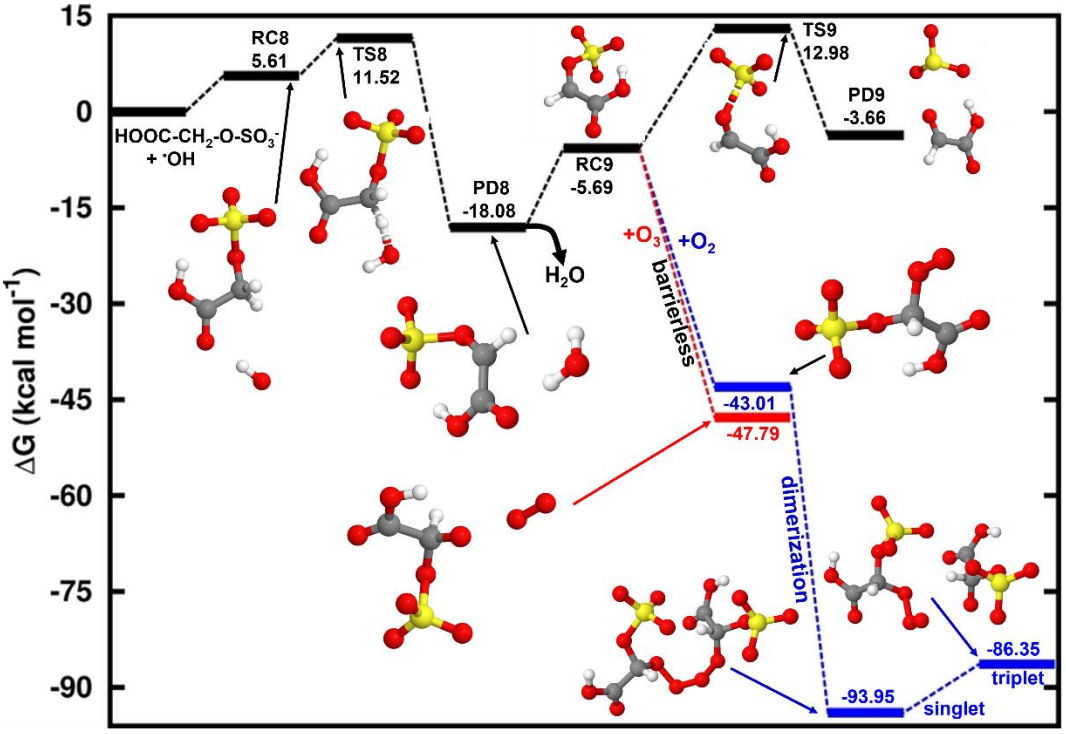

Figure 7: Gibbs free energy changes (in kcal mol^{-1}) and optimized structures for all stationary states in the reaction of HOOC-CH$_2$-O-SO$_3^-$ with HO• radicals, and subsequent reaction of the intermediate reactant complex with O$_3$ (red line) and O$_2$ (blue line). The sulfur atom is yellow, the oxygen atom is red, the carbon atom is grey and the hydrogen atom is white color.

Another reaction pathway for HOOC-CH•-O-SO$_3^-$ reaction is by O$_2$ addition (**reaction (R11)**) in a barrierless process to form a peroxyl radical (HOOC-CH(OO•)-O-SO$_3^-$) with the release of 43.01 kcal mol^{-1} Gibbs free energy. HOOC-CH(OO•)-O-SO$_3^-$ can recombine with each other to form a tetroxide (O$_3^-$S-O-CH(COOH)-OOOO-CH(COOH)-O-SO$_3^-$) as shown in **Figure 7**. However, we found that contrary to the case of •OO-CH$_2$-O-SO$_3^-$ where the tetroxide could readily decompose to form the •O-CH$_2$-O-SO$_3^-$ radical in the singlet state, the fragmentation of O$_3^-$S-O-CH(COOH)-OOOO-CH(COOH)-O-SO$_3^-$ to form the alkoxyl radical HOOC-CH(O)•-O-SO$_3^-$ occurred on the triplet state instead. The triplet electronic state was shown from a recent study to be favorable to the decomposition of tetroxides to alkoxyl radicals from some atmospherically relevant peroxyl radicals (Salo et al., 2022). **Figure S6(B)** clearly shows the antibonding orbitals in the triplet state prior to the formation of HOOC-CH(O)•-O-SO$_3^-$ upon which rests the unpaired electron.

3.3 Atmospheric Implication

Organosulfates are important organic tracers for aerosols in the atmosphere. Although sufficient information on their sources and abundance has been gathered from previous studies, the understanding of the mechanisms of their transformation in the atmosphere remains incomplete. By investigating the decomposition mechanisms of two small atmospheric organosulfates

(methyl sulfate and glycolic acid sulfate) by reaction with HO• radicals in this study, it was shown that the reaction of glycolic acid sulfate in the gas-phase is more kinetically favorable than that of methyl sulfate, which can be attributed to the effect of -COOH substitution that stabilizes the intermediate reactant complex from glycolic acid. The chemical transformation of both organosulfates was seen to be more effective in the aqueous-phase, with the reaction of methyl sulfate being more extensive than that of glycolic acid sulfate. The main products of these transformations are carbonyl compounds and inorganic sulfate for which detailed mechanisms are provided. Not only does this study clarify the effect of substituents on the fragmentation of organosulfates, but it also complements previous experimental observations on methyl sulfate oxidation by HO• radicals (Kwong et al., 2018). For this reaction, we obtained a rate constant of 1.14×10^{-13} cm^3 $molecule^{-1}$ s^{-1} in the gas-phase, in agreement with the previously reported experimental value ($(3.79 \pm 0.19) \times10^{-13}$ cm^3 $moelcule^{-1}$ s^{-1}) (Kwong et al., 2018). We also report a rate bimolecular rate constant of 6.17×10^{-12} cm^3 $molecule^{-1}$ s^{-1} for the gas-phase reaction of HO• reaction with glycolic acid at 298.15 K. In the aqueous-phase, we determined rate constants of 7.87×10^{6} $M^{-1}s^{-1}$ and 7.29×10^{8} $M^{-1}s^{-1}$ for the reaction of methyl sulfate and glycolic acid sulfate, respectively.

Among the three processes investigated (self-decomposition, reaction with O_3 and reaction with O_2), alkoxyl radicals can be formed from reactions with both O_2 and O_3, with the reaction with O_2 being the most kinetically favorable. From the discussion above, we clarify that the reaction with O_3 is a key intermediate step in the formation of alkoxy radicals that further decompose to inorganic sulfate and carbonyl compounds. It is speculated that under most atmospherically relevant conditions, the formation of intermediate alkoxyl radicals from O_3 reactions in the oxidation of organosulfates would readily complement previous reported Bennett and Summers mechanisms (Bennett and Summers, 1974) that involve reactions with O_2. It should, however, be noted that the overall rate of the reaction with O_2 can be higher than that of the reaction with O_3 due to the high atmospheric concentration of O_2.

Overall, the kinetics results show a moderate difference between the rate constants of HO• reactions with methyl sulfate and glycolic acid sulfate. The slightly high rate constant of the reaction of glycolic acid sulfate indicate the enhancing effect of the -COOH group in the hydrogen abstraction by HO•. Moreover, we found that the hydrogen abstraction from the -COOH group in glycolic acid sulfate leads to decarboxylation and eventually forms similar products as methyl sulfate. It can be inferred that for organosulfates having a carboxyl substituent at the β-position relatiove to the sulfate group, decarboxylation would be take place, leading to the formation of the corresponding alkyl sulfate radical. This highlights the potential role that chemical substitution on the carbon chain of organosulfates may play during their decomposition. Given the high variety of organosulfates detected in atmospheric particles, it is necessary to deeply evaluate the role of molecular structures in their chemical transformation in order to guarantee proper understanding of their impact on the chemical composition of aerosols. A general trend of the effect of chemical substitution can be obtained from segregated studies of the chemical transformation of different classes of organosulfates derived from anthropogenic and biogenic precursors.

Data availability

All data from this research can be obtained upon request by contacting the corresponding author.

Author contributions

Conceptualization: NTT; Funding acquisition: NTT and LD; Investigation: LX and NTT; Supervision: LD; Writing – original draft preparation: LX and NTT. Writing – review & editing: SNT, JNG, and LD.

Competing interests

The authors declare that they have no conflict of interest.

Acknowledgements

The authors acknowledge the Wuxi Hengding Supercomputing Center Co., LTD and National Supercomputer Center in Tianjin for providing the computational resources. We thank Kristian H. Møller and Rasmus V. Otkjær of the University of Copenhagen for providing the script to calculate the Eckart tunneling correction.

Financial support

This work was supported by National Key Research and Development Program of China (2023YFC3706203), National Natural Science Foundation of China (22376121), and Natural Science Foundation of Shandong Province (ZR2023MD041).

References

An, G.-C.: Enhancement of atmospheric nucleation precursors on formic sulfuric anhydride induced nucleation: Theoretical mechanism, Chemosphere, 368, 143684, 10.1016/j.chemosphere.2024.143684, 2024.

Bennett, J. E. and Summers, R.: Product Studies of the Mutual Termination Reactions of sec-Alkylperoxy Radicals: Evidence for Non-Cyclic Termination, Can. J. Chem., 52, 1377-1379, 10.1139/v74-209, 1974.

Bork, N., Kurtén, T., and Vehkamäki, H.: Exploring the atmospheric chemistry of $O_2SO_3^-$ and assessing the maximum turnover number of ion-catalysed H_2SO_4 formation, Atmos. Chem. Phys., 13, 3695-3703, 10.5194/acp-13-3695-2013, 2013.

Bork, N., Kurtén, T., Enghoff, M., Pedersen, J. O. P., Mikkelsen, K. V., and Svensmark, H.: Structures and reaction rates of the gaseous oxidation of SO_2 by an $O_3^-(H_2O)_{0-5}$ cluster–a density functional theory investigation, Atmos. Chem. Phys., 12, 3639-3652, 10.5194/acp-12-3639-2012, 2012.

Buehler, R. E., Staehelin, J., and Hoigne, J.: Ozone decomposition in water studied by pulse radiolysis. 1. Perhydroxyl (HO_2)/hyperoxide (O_2-) and HO_3/O_3^- as intermediates, J. Phys. Chem., 88, 2560-2564, 10.1021/j150656a026, 1984.

Buhler, R., Staehelin, J., and Hoigne, J.: Ozone Decomposition in Water Studied by Pulse Radiolysis 1. HO_2/O_2^- and HO_3/O_3^- as Intermediates - Correction, J. Phys. Chem., 8, 5450-5450, 10.1021/j150666a600, 1984.

Buxton, G. V., Greenstock, C. L., Helman, W. P., and Ross, A. B.: Critical Review of rate constants for reactions of hydrated electrons, hydrogen atoms and hydroxyl radicals ($\cdot OH/\cdot O^-$) in Aqueous Solution, J. Phys. Chem. Ref. Data, 17, 513-886, 10.1063/1.555805, 1988.

Cai, D., Wang, X., Chen, J., and Li, X.: Molecular Characterization of Organosulfates in Highly Polluted Atmosphere Using Ultra-High-Resolution Mass Spectrometry, J. Geophys. Res.-Atmos., 125, e2019JD032253, 10.1029/2019JD032253, 2020.

Chan, M. N., Surratt, J. D., Chan, A. W. H., Schilling, K., Offenberg, J. H., Lewandowski, M., Edney, E. O., Kleindienst, T. E., Jaoui, M., Edgerton, E. S., Tanner, R. L., Shaw, S. L., Zheng, M., Knipping, E. M., and Seinfeld, J. H.: Influence of aerosol acidity on the chemical composition of secondary organic aerosol from β-caryophyllene, Atmos. Chem. Phys., 11, 1735-1751, 10.5194/acp-11-1735-2011, 2011.

Cheng, J., Yue, L., Hua, J., Dong, H., Li, Y.-Y., Zhou, J., and Lin, R.: Hydrothermal heating with sulphuric acid contributes to improved fermentative hydrogen and methane co-generation from Dianchi Lake algal bloom, Energ. Convers. Manage., 192, 282-291, 10.1016/j.enconman.2019.04.003, 2019.

Cheng, Y., Wang, R., Chen, Y., Tian, S., Gao, N., Zhang, Z., and Zhang, T.: Hydrolysis of SO_3 in Small Clusters of Sulfuric Acid: Mechanistic and Kinetic Study, ACS Earth and Space Chem., 6, 3078-3089, 10.1021/acsearthspacechem.2c00290, 2022.

Collins, F. C. and Kimball, G. E.: Diffusion-controlled reaction rates, J. Colloid Sci., 4, 425-437, 10.1016/0095-8522(49)90023-9, 1949.

Ding, C., Cheng, Y., Wang, H., Yang, J., Li, Z., Lily, M., Wang, R., and Zhang, T.: Determination of the influence of water on the SO_3 + CH_3OH reaction in the gas phase and at the air–water interface, Phys. Chem. Chem. Phys., 25, 15693-15701, 10.1039/D3CP01245J, 2023.

Eckart, C.: The Penetration of a Potential Barrier by Electrons, Phys. Rev. 35, 1303-1309, 10.1103/PhysRev.35.1303, 1930.

Ehn, M., Junninen, H., Petaja, T., Kurten, T., Kerminen, V. M., Schobesberger, S., Manninen, H. E., Ortega, I. K., Vehkamaki, H., Kulmala, M., and Worsnop, D. R.: Composition and temporal behavior of ambient ions in the boreal forest, Atmos. Chem. Phys., 10, 8513-8530, 10.5194/acp-10-8513-2010, 2010.

Einstein, A.: Über die von der molekularkinetischen Theorie der Wärme geforderte Bewegung von in ruhenden Flüssigkeiten suspendierten Teilchen, Ann. Phys., 322, 549-560, 10.1002/andp.19053220806, 1905.

Enghoff, M. and Svensmark, H.: The role of atmospheric ions in aerosol nucleation–a review, Atmos. Chem. Phys., 8, 4911-4923, 10.5194/acp-8-4911-2008, 2008.

England, C. and Corcoran, W. H.: Kinetics and Mechanisms of the Gas-Phase Reaction of Water Vapor and Nitrogen Dioxide, Industrial & Engineering Chemistry Fundamentals, 13, 373-384, 10.1021/i160052a014, 1974.

Estillore, A. D., Hettiyadura, A. P., Qin, Z., Leckrone, E., Wombacher, B., Humphry, T., Stone, E. A., and Grassian, V. H.: Water Uptake and Hygroscopic Growth of Organosulfate Aerosol, Environ. Sci. Technol, 50, 4259-4268, 10.1021/acs.est.5b05014, 2016.

Fehsenfeld, F. and Ferguson, E.: Laboratory studies of negative ion reactions with atmospheric trace constituents, J. Chem. Phys., 61, 3181-3193, 10.1063/1.1682474, 1974.

Ford, P. C. and Miranda, K. M.: The solution chemistry of nitric oxide and other reactive nitrogen species, Nitric Oxide, 103, 31-46, 10.1016/j.niox.2020.07.004, 2020.

Frisch, M. J., Trucks, G. W., Schlegel, H. B., Scuseria, G. E., Robb, M. A., Cheeseman, J. R., Scalmani, G., Barone, V., Petersson, G. A., Nakatsuji, H., Li, X., Caricato, M., Marenich, A. V., Bloino, J., Janesko, B. G., Gomperts, R., Mennucci, B., Hratchian, H. P., Ortiz, J. V., Izmaylov, A. F., Sonnenberg, J. L., Williams, Ding, F., Lipparini, F., Egidi, F., Goings, J., Peng, B., Petrone, A., Henderson, T., Ranasinghe, D., Zakrzewski, V. G., Gao, J., Rega, N., Zheng, G., Liang, W., Hada, M., Ehara, M., Toyota, K., Fukuda, R., Hasegawa, J., Ishida, M., Nakajima, T., Honda, Y., Kitao, O., Nakai, H., Vreven, T., Throssell, K., Montgomery Jr., J. A., Peralta, J. E., Ogliaro, F., Bearpark, M. J., Heyd, J. J., Brothers, E. N., Kudin, K. N., Staroverov, V. N., Keith, T. A., Kobayashi, R., Normand, J., Raghavachari, K., Rendell, A. P., Burant, J. C., Iyengar, S. S., Tomasi, J., Cossi, M., Millam, J. M., Klene, M., Adamo, C., Cammi, R., Ochterski, J. W., Martin, R. L., Morokuma, K., Farkas, O., Foresman, J. B., and Fox, D. J.: Gaussian 09 Rev. E.01, Wallingford, CT, 2013.

George, I. J. and Abbatt, J. P. D.: Heterogeneous oxidation of atmospheric aerosol particles by gas-phase radicals, Nature Chem., 2, 713-722, 10.1038/nchem.806, 2010.

Ghigo, G., Maranzana, A., and Tonachini, G.: Combustion and atmospheric oxidation of hydrocarbons: Theoretical study of the methyl peroxyl self-reaction, J. Chem. Phys., 118, 10575-10583, 10.1063/1.1574316, 2003.

Gweme, D. T. and Styler, S. A.: OH Radical Oxidation of Organosulfates in the Atmospheric Aqueous Phase, J. Phys. Chem. A, 128, 9462-9475, 10.1021/acs.jpca.4c02877, 2024.

Hallquist, M., Wenger, J. C., Baltensperger, U., Rudich, Y., Simpson, D., Claeys, M., Dommen, J., Donahue, N. M., George, C., Goldstein, A. H., Hamilton, J. F., Herrmann, H., Hoffmann, T., Iinuma, Y., Jang, M., Jenkin, M. E., Jimenez, J. L., Kiendler-Scharr, A., Maenhaut, W., McFiggans, G., Mentel, T. F., Monod, A., Prevot, A. S. H., Seinfeld, J. H., Surratt, J. D., Szmigielski, R., and Wildt, J.: The formation, properties and impact of secondary organic aerosol: current and emerging issues, Atmos. Chem. Phys., 9, 5155-5236, 10.5194/acp-9-5155-2009, 2009.

Heindel, J. P., Yu, Q., Bowman, J. M., and Xantheas, S. S.: Benchmark Electronic Structure Calculations for $H_3O^+(H_2O)_n$, n = 0–5, Clusters and Tests of an Existing 1,2,3-Body Potential Energy Surface with a New 4-Body Correction, J. Chem. Theory Comput., 14, 4553-4566, 10.1021/acs.jctc.8b00598, 2018.

Hettiyadura, A. P. S., Stone, E. A., Kundu, S., Baker, Z., Geddes, E., Richards, K., and Humphry, T.: Determination of atmospheric organosulfates using HILIC chromatography with MS detection, Atmos. Meas. Tech., 8, 2347-2358, 10.5194/amt-8-2347-2015, 2015.

Hettiyadura, A. P. S., Jayarathne, T., Baumann, K., Goldstein, A. H., de Gouw, J. A., Koss, A., Keutsch, F. N., Skog, K., and Stone, E. A.: Qualitative and quantitative analysis of atmospheric organosulfates in Centreville, Alabama, Atmos. Chem. Phys., 17, 1343-1359, 10.5194/acp-17-1343-2017, 2017.

Hofmann-Sievert, R. and Castleman, A. W., Jr.: Reaction of sulfur trioxide with water clusters and the formation of sulfuric acid, J. Phys. Chem., 88, 3329-3333, 10.1021/j150659a038, 1984.

Hofmann, M. and Schleyer, P. v. R.: Acid Rain: Ab Initio Investigation of the $H_2O{\bullet}SO_3$ Complex and Its Conversion to H_2SO_4, J. Am. Chem. Soc., 116, 4947-4952, 10.1021/ja00090a045, 1994.

Huang, D. D., Li, Y. J., Lee, B. P., and Chan, C. K.: Analysis of Organic Sulfur Compounds in Atmospheric Aerosols at the HKUST Supersite in Hong Kong Using HR-ToF-AMS, Environ. Sci. Technol., 49, 3672-3679, 10.1021/es5056269, 2015.

Huang, R. J., Cao, J., Chen, Y., Yang, L., Shen, J., You, Q., Wang, K., Lin, C., Xu, W., Gao, B., Li, Y., Chen, Q., Hoffmann, T., O'Dowd, C. D., Bilde, M., and Glasius, M.: Organosulfates in atmospheric aerosol: synthesis and quantitative analysis of PM2.5 from Xi'an, northwestern China, Atmos. Meas. Tech., 11, 3447-3456, 10.5194/amt-11-3447-2018, 2018.

Hughes, D. D. and Stone, E. A.: Organosulfates in the Midwestern United States: abundance, composition and stability, J. Environ. Chem., 16, 312-322, 10.1071/EN18260, 2019.

Iinuma, Y., Müller, C., Böge, O., Gnauk, T., and Herrmann, H.: The formation of organic sulfate esters in the limonene ozonolysis secondary organic aerosol (SOA) under acidic conditions, Atmos. Env., 41, 5571-5583, 10.1016/j.atmosenv.2007.03.007, 2007.

Jensen, S. K., Keiding, S. R., and Thøgersen, J.: The hunt for HCO(aq), Phys. Chem. Chem. Phys., 12, 8926-8933, 10.1039/B924902H, 2010.

Kourtchev, I., Godoi, R. H. M., Connors, S., Levine, J. G., Archibald, A. T., Godoi, A. F. L., Paralovo, S. L., Barbosa, C. G. G., Souza, R. A. F., Manzi, A. O., Seco, R., Sjostedt, S., Park, J. H., Guenther, A., Kim, S., Smith, J., Martin, S. T., and Kalberer, M.: Molecular composition of organic aerosols in central Amazonia: an ultra-high-resolution mass spectrometry study, Atmos. Chem. Phys., 16, 11899-11913, 10.5194/acp-16-11899-2016, 2016.

Kwong, K. C., Chim, M. M., Davies, J. F., Wilson, K. R., and Chan, M. N.: Importance of sulfate radical anion formation and chemistry in heterogeneous OH oxidation of sodium methyl sulfate, the smallest organosulfate, Atmos. Chem. Phys., 18, 2809-2820, 10.5194/acp-18-2809-2018, 2018.

Larson, L. J., Kuno, M., and Tao, F.-M.: Hydrolysis of sulfur trioxide to form sulfuric acid in small water clusters, J. Chem. Phys., 112, 8830-8838, 2000.

Le Breton, M., Wang, Y., Hallquist, Å. M., Pathak, R. K., Zheng, J., Yang, Y., Shang, D., Glasius, M., Bannan, T. J., Liu, Q., Chan, C. K., Percival, C. J., Zhu, W., Lou, S., Topping, D., Wang, Y., Yu, J., Lu, K., Guo, S., Hu, M., and Hallquist, M.: Online gas- and particle-phase measurements of organosulfates, organosulfonates and nitrooxy organosulfates in Beijing utilizing a FIGAERO ToF-CIMS, Atmos. Chem. Phys., 18, 10355-10371, 10.5194/acp-18-10355-2018, 2018.

Lee, Y. N. and Schwartz, S. E.: Reaction kinetics of nitrogen dioxide with liquid water at low partial pressure, J. Phys. Chem., 85, 840-848, 10.1021/j150607a022, 1981.

Liang, Y.-N., Li, J., Wang, Q.-D., Wang, F., and Li, X.-Y.: Computational Study of the Reaction Mechanism of the Methylperoxy Self-Reaction, J. Phys. Chem. A, 115, 13534-13541, 10.1021/jp2048508, 2011.

Liao, J., Froyd, K. D., Murphy, D. M., Keutsch, F. N., Yu, G., Wennberg, P. O., St. Clair, J. M., Crounse, J. D., Wisthaler, A., Mikoviny, T., Jimenez, J. L., Campuzano-Jost, P., Day, D. A., Hu, W., Ryerson, T. B., Pollack, I. B., Peischl, J., Anderson, B. E., Ziemba, L. D., Blake, D. R., Meinardi, S., and Diskin, G.: Airborne measurements of organosulfates over the continental U.S, J. Geophys. Res.-Atmos., 120, 2990-3005, 10.1002/2014JD022378, 2015.

Lin, Y.-H., Budisulistiorini, S. H., Chu, K., Siejack, R. A., Zhang, H., Riva, M., Zhang, Z., Gold, A., Kautzman, K. E., and Surratt, J. D.: Light-Absorbing Oligomer Formation in Secondary Organic Aerosol from Reactive Uptake of Isoprene Epoxydiols, Environ. Sci. Technol., 48, 12012-12021, 10.1021/es503142b, 2014.

Loerting, T. and Liedl, K. R.: Toward elimination of discrepancies between theory and experiment: The rate constant of the atmospheric conversion of SO_3 to H_2SO_4, Proc. Natl Acad. Sci., 97, 8874-8878, 10.1073/pnas.97.16.8874, 2000.

Lovato, M. E., Martín, C. A., and Cassano, A. E.: A reaction kinetic model for ozone decomposition in aqueous media valid for neutral and acidic pH, Chem. Eng. J., 146, 486-497, 10.1016/j.cej.2008.11.001, 2009.

Lu, T. and Chen, F.: Multiwfn: A multifunctional wavefunction analyzer, J. Comput. Chem., 33, 580-592, 10.1002/jcc.22885, 2012.

Markovitch, O. and Agmon, N.: Structure and Energetics of the Hydronium Hydration Shells, J. Phys. Chem. A, 111, 2253-2256, 10.1021/jp068960g, 2007.

Morokuma, K. and Muguruma, C.: Ab initio Molecular Orbital Study of the Mechanism of the Gas Phase Reaction SO_3 + H_2O: Importance of the Second Water Molecule, J. Am. Chem. Soc., 116, 10316-10317, 10.1021/ja00101a068, 1994.

Nangia, P. S. and Benson, S. W.: The kinetics of the interaction of peroxy radicals. II. Primary and secondary alkyl peroxy, Int. J. Chem. Kinet., 12, 43-53, 10.1002/kin.550120105, 1980.

Nguyen, Q. T., Christensen, M. K., Cozzi, F., Zare, A., Hansen, A. M. K., Kristensen, K., Tulinius, T. E., Madsen, H. H., Christensen, J. H., Brandt, J., Massling, A., Nøjgaard, J. K., and Glasius, M.: Understanding the anthropogenic influence on formation of biogenic secondary organic aerosols in Denmark via analysis of organosulfates and related oxidation products, Atmos. Chem. Phys., 14, 8961-8981, 10.5194/acp-14-8961-2014, 2014.

Noziere, B., Ekstrom, S., Alsberg, T., and Holmstrom, S.: Radical-initiated formation of organosulfates and surfactants in atmospheric aerosols, Geophys. Res. Let., 37, 10.1029/2009gl041683, 2010.

Nozière, B., Kalberer, M., Claeys, M., Allan, J., D'Anna, B., Decesari, S., Finessi, E., Glasius, M., Grgić, I., Hamilton, J. F., Hoffmann, T., Iinuma, Y., Jaoui, M., Kahnt, A., Kampf, C. J., Kourtchev, I., Maenhaut, W., Marsden, N., Saarikoski, S., Schnelle-Kreis, J., Surratt, J. D., Szidat, S., Szmigielski, R., and Wisthaler, A.: The Molecular Identification of Organic Compounds in the Atmosphere: State of the Art and Challenges, Chem. Rev., 115, 3919-3983, 10.1021/cr5003485, 2015.

Ostovari, H., Zahedi, E., Sarvi, I., and Shiroudi, A.: Kinetic and mechanistic insight into the formation of amphetamine using the Leuckart–Wallach reaction and interaction of the drug with GpC·CpG base-pair step of DNA: a DFT study, Monatsh. Chem., 149, 1045-1057, 10.1007/s00706-018-2145-7, 2018.

Passananti, M., Kong, L., Shang, J., Dupart, Y., Perrier, S., Chen, J., Donaldson, D. J., and George, C.: Organosulfate Formation through the Heterogeneous Reaction of Sulfur Dioxide with Unsaturated Fatty Acids and Long-Chain Alkenes, Angew. Chem. Int. Ed., 55, 10336-10339, 10.1002/anie.201605266, 2016.

Peng, C., Razafindrambinina, P. N., Malek, K. A., Chen, L., Wang, W., Huang, R. J., Zhang, Y., Ding, X., Ge, M., Wang, X., Asa-Awuku, A. A., and Tang, M.: Interactions of organosulfates with water vapor under sub- and supersaturated conditions, Atmos. Chem. Phys., 21, 7135-7148, 10.5194/acp-21-7135-2021, 2021.

Riplinger, C. and Neese, F.: An efficient and near linear scaling pair natural orbital based local coupled cluster method, J. Chem. Phys., 138, 034106, 10.1063/1.4773581, 2013.

Rudziński, K. J., Gmachowski, L., and Kuznietsova, I.: Reactions of isoprene and sulphoxy radical-anions – a possible source of atmospheric organosulphites and organosulphates, Atmos. Chem. Phys., 9, 2129-2140, 10.5194/acp-9-2129-2009, 2009.

Russell, G. A.: Deuterium-isotope Effects in the Autoxidation of Aralkyl Hydrocarbons. Mechanism of the Interaction of PEroxy Radicals1, J. Am. Chem. Soc., 79, 3871-3877, 10.1021/ja01571a068, 1957.

Salo, V.-T., Valiev, R., Lehtola, S., and Kurtén, T.: Gas-Phase Peroxyl Radical Recombination Reactions: A Computational Study of Formation and Decomposition of Tetroxides, J. Phys. Chem. A, 126, 4046-4056, 10.1021/acs.jpca.2c01321, 2022.

Seinfeld, J. H. and Pandis, S. N.: Atmospheric Chemistry and Physics: From Air Pollution to Climate Change, John Wiley & Sons, New York, 88 pp., 10.1063/1.882420, 1998.

Shang, J., Passananti, M., Dupart, Y., Ciuraru, R., Tinel, L., Rossignol, S., Perrier, S., Zhu, T., and George, C.: SO_2 Uptake on Oleic Acid: A New Formation Pathway of Organosulfur Compounds in the Atmosphere, Environ. Sci. Technol. Lett., 3, 67-72, 10.1021/acs.estlett.6b00006, 2016.

Smoluchowski M, V.: Mathematical Theory of the Kinetics of the Coagulation of Colloidal Solutions, Z. Phys. Chem., 92, 129-168, 1917.

Staehelin, J. and Hoigne, J.: Decomposition of ozone in water: rate of initiation by hydroxide ions and hydrogen peroxide, Environ. Sci. Technol., 16, 676-681, 10.1021/es00104a009, 1982.

Staehelin, J., Buehler, R. E., and Hoigne, J.: Ozone decomposition in water studied by pulse radiolysis. 2. Hydroxyl and hydrogen tetroxide (HO4) as chain intermediates, J. Phys. Chem., 88, 5999-6004, 10.1021/j150668a051, 1984.

Stone, E. A., Yang, L., Yu, L. E., and Rupakheti, M.: Characterization of organosulfates in atmospheric aerosols at Four Asian locations, Atmos. Env., 47, 323-329, 10.1016/j.atmosenv.2011.10.058, 2012.

Surratt, J. D., Gomez-Gonzalez, Y., Chan, A. W. H., Vermeylen, R., Shahgholi, M., Kleindienst, T. E., Edney, E. O., Offenberg, J. H., Lewandowski, M., Jaoui, M., Maenhaut, W., Claeys, M., Flagan, R. C., and Seinfeld, J. H.: Organosulfate formation in biogenic secondary organic aerosol, J. Phys. Chem. A, 112, 8345-8378, 10.1021/jp802310p, 2008.

Svensmark, H., Pedersen, J. O. P., Marsh, N. D., Enghoff, M. B., and Uggerhoj, U. I.: Experimental evidence for the role of ions in particle nucleation under atmospheric conditions, Proc. R. Soc. A: Math. Phys. Eng. Sci., 463, 385-396, 10.1098/rspa.2006.1773, 2007.

Tan, S. P. and Piri, M.: Modeling the Solubility of Nitrogen Dioxide in Water Using Perturbed-Chain Statistical Associating Fluid Theory, Ind. Eng. Chem. Res., 52, 16032-16043, 10.1021/ie402417p, 2013.

Truhlar, D. G.: Nearly encounter-controlled reactions: The equivalence of the steady-state and diffusional viewpoints, J. Chem. Educ., 62, 104, 10.1021/ed062p104, 1985.

Truhlar, D. G., Garrett, B. C., and Klippenstein, S. J.: Current Status of Transition-State Theory, J. Phys. Chem., 100, 12771-12800, 10.1021/jp953748q, 1996.

Tsona, N. T. and Du, L.: Hydration of glycolic acid sulfate and lactic acid sulfate: Atmospheric implications, Atmos. Env., 216, 116921, 10.1016/j.atmosenv.2019.116921, 2019a.

Tsona, N. T. and Du, L.: A potential source of atmospheric sulfate from O_2^--induced SO_2 oxidation by ozone, Atmos. Chem. Phys., 19, 649-661, 10.5194/acp-19-649-2019, 2019b.

Wang, R., Kang, J., Zhang, S., Shao, X., Jin, L., Zhang, T., and Wang, Z.: Catalytic effect of $(H_2O)_n$ (n=1–2) on the hydrogen abstraction reaction of H_2O_2+HS→H_2S+HO_2 under tropospheric conditions, Comput. Theor. Chem., 1110, 25-34, 10.1016/j.comptc.2017.03.045, 2017.

Wang, R., Cheng, Y., Chen, S., Li, R., Hu, Y., Guo, X., Zhang, T., Song, F., and Li, H.: Reaction of SO_3 with H_2SO_4 and its implications for aerosol particle formation in the gas phase and at the air–water interface, Atmos. Chem. Phys., 24, 4029-4046, 10.5194/acp-24-4029-2024, 2024.

Wang, R., Yao, Q., Wen, M., Tian, S., Wang, Y., Wang, Z., Yu, X., Shao, X., and Chen, L.: Catalytic effect of $(H_2O)_n$ (n = 1–3) clusters on the HO_2 + SO_2 → HOSO + $^3O_2$ reaction under tropospheric conditions, RSC Adv., 9, 16195-16207, 10.1039/C9RA00169G, 2019.

Wang, Y., Zhao, Y., Wang, Y., Yu, J. Z., Shao, J., Liu, P., Zhu, W., Cheng, Z., Li, Z., Yan, N., and Xiao, H.: Organosulfates in atmospheric aerosols in Shanghai, China: seasonal and interannual variability, origin, and formation mechanisms, Atmos. Chem. Phys., 21, 2959-2980, 10.5194/acp-21-2959-2021, 2021.

Worton, D. R., Goldstein, A. H., Farmer, D. K., Docherty, K. S., Jimenez, J. L., Gilman, J. B., Kuster, W. C., de Gouw, J., Williams, B. J., Kreisberg, N. M., Hering, S. V., Bench, G., McKay, M., Kristensen, K., Glasius, M., Surratt, J. D., and Seinfeld, J. H.: Origins and composition of fine atmospheric carbonaceous aerosol in the Sierra Nevada Mountains, California, Atmos. Chem. Phys., 11, 10219-10241, 10.5194/acp-11-10219-2011, 2011.

Xu, L. and Coote, M. L.: Methods To Improve the Calculations of Solvation Model Density Solvation Free Energies and Associated Aqueous pKa Values: Comparison between Choosing an Optimal Theoretical Level, Solute Cavity Scaling, and Using Explicit Solvent Molecules, J. Phys. Chem. A, 123, 7430-7438, 10.1021/acs.jpca.9b04920, 2019.

Xu, R., Ng, S. I. M., Chow, W. S., Wong, Y. K., Wang, Y., Lai, D., Yao, Z., So, P. K., Yu, J. Z., and Chan, M. N.: Chemical transformation of α-pinene-derived organosulfate via heterogeneous OH oxidation: implications for sources and environmental fates of atmospheric organosulfates, Atmos. Chem. Phys., 22, 5685-5700, 10.5194/acp-22-5685-2022, 2022.

Zhang, P., Wang, W., Zhang, T., Chen, L., Du, Y., Li, C., and Lü, J.: Theoretical Study on the Mechanism and Kinetics for the Self-Reaction of $C_2H_5O_2$ Radicals, J. Phys. Chem. A, 116, 4610-4620, 10.1021/jp301308u, 2012.
Zhang, X., Lian, Y., Tan, S., and Yin, S.: Organosulfate produced from consumption of SO_3 speeds up sulfuric acid–dimethylamine atmospheric nucleation, Atmos. Chem. Phys., 24, 3593-3612, 10.5194/acp-24-3593-2024, 2024.
Zhao, Y. and Truhlar, D. G.: The M06 suite of density functionals for main group thermochemistry, thermochemical kinetics, noncovalent interactions, excited states, and transition elements: two new functionals and systematic testing of four M06-class functionals and 12 other functionals, Theor. Chem. Acc., 120, 215-241, 10.1007/s00214-007-0310-x, 2008.